Resting-State Functional Connectivity of the Subthalamic Nucleus to Limbic, Associative, and Motor Networks

Sheeba Arnold Anteraper,[1,2] Xavier Guell,[3,4] Susan Whitfield-Gabrieli,[1,3]
Christina Triantafyllou,[5] Aaron T. Mattfeld,[6] John D. Gabrieli,[1,3] and Maiya R. Geddes[1,3,7]

Abstract

The subthalamic nucleus (STN) is a small structure situated deep in the midbrain that exhibits wide-ranging functionality. In addition to its role in motor control, the STN is considered a hub for synchronizing aspects of emotion and cognition including attention, inhibitory control, motivation, and working memory. Evidence from neuroanatomical tracer studies suggests that the medial, ventromedial, and dorsolateral parts of the STN correspond to limbic, associative, and motor subdivisions, respectively. Although the extent of STN functional anatomical overlap remains unclear, blood oxygenation level dependent imaging of the STN may provide complementary information about the diverse functions of this structure. Methodological limitations in spatial and temporal resolutions, however, have prevented a comprehensive exploration of temporal correlations from the STN to the whole brain. In this study, we optimize spatial (2 mm isotropic) and temporal (TR = 1 s) resolutions to take full advantage of the time series signal-to-noise ratio capabilities of multichannel array coils and simultaneous multislice imaging. We interrogated STN seed-to-voxel resting-state functional MRI connectivity in a group of 30 healthy participants that included the whole brain at high-temporal and spatial resolutions. This analysis revealed STN functional connectivity to limbic, associative, and motor networks. Our findings contribute to the understanding of STN functional neuroanatomy in humans and are clinically relevant for ongoing research in deep brain stimulation.

Keywords: subthalamic nucleus, 32 channel coil, functional connectivity, resting-state networks, deep brain stimulation

Introduction

THE SUBTHALAMIC NUCLEUS (STN) is a small biconvex lens-shaped nucleus located ventral to the thalamus that is functionally grouped with the basal ganglia. Structural MRI studies report the intercomissural distance of this structure as 26.3 mm, with length, width, and through plane dimensions of 7.7 mm, 6 mm, and 8.5 mm, respectively (Mavridis et al., 2013). The functional heterogeneity of this deep gray matter (GM) structure was apparent in early descriptions of patients with STN damage: patients developed motor symptoms (hemiballismus) coupled with impulsivity and disturbances in emotional regulation (Martin, 1927). Primate tracer studies have shown that the STN is a convergence zone of cortical projections from functionally diverse limbic, associative, and motor regions (Haynes and Haber, 2013). These anatomical considerations have important clinical relevance: high-frequency deep brain stimulation (DBS) of the STN is a favored surgical treatment for advanced Parkinson's disease (PD). Although this intervention improves dopaminergic drug-sensitive motor symptoms, it can result in adverse neurocognitive and behavioral effects (Benabid et al., 2009). Neuropsychiatric complications of DBS include depression, apathy syndrome, anxiety disorders, (hypo)mania, personality change, hypersexuality, aggressive behavior, and rare reports of suicide (Benabid

[1]A.A. Martinos Imaging Center, McGovern Institute for Brain Research, Massachusetts Institute of Technology, Cambridge, Massachusetts.
[2]Alan and Lorraine Bressler Clinical and Research Program for Autism Spectrum Disorder, Massachusetts General Hospital, Boston, Massachusetts.
[3]Department of Brain and Cognitive Sciences, Massachusetts Institute of Technology, Cambridge, Massachusetts.
[4]Cognitive Neuroscience Research Unit (URNC), Department of Psychiatry and Forensic Medicine, Universitat Autonoma de Barcelona, Barcelona, Spain.
[5]Department of Radiology, A.A. Martinos Center for Biomedical Imaging, Massachusetts General Hospital, Harvard Medical School, Charlestown, Massachusetts.
[6]Department of Psychology, Florida International University, Miami, Florida.
[7]Division of Cognitive and Behavioral Neurology, Brigham and Women's Hospital, Harvard University, Boston, Massachusetts.

et al., 2009; Mallet et al., 2007; Scangos and Shahlaie, 2017; Temel et al., 2006; Ulla et al., 2011; Voon et al., 2008).

Cognitive side effects after STN DBS are frequent and include reduced word fluency and executive dysfunction (Temel et al., 2006; Witt et al., 2008). Intraoperative microrecordings in PD patients have shown single-neuron firing within STN during motivational and emotional processes (Sieger et al., 2015). Stimulation at dorsal and ventral electrode contacts has shown separable effects on motor and emotional functions in PD (Greenhouse et al., 2011). A positron emission tomography (PET) study of two patients with PD who experienced transient hypomania after anteromedial STN stimulation has shown concomitant activations in cortical and thalamic regions involved in processing limbic and associative information (Mallet el al., 2007). Together these findings suggest that STN plays a key role in the motor, cognitive, and emotional integration of behavior. As reaffirmed by quantitative analysis of tractography-based activation models (Hartmann et al., 2015), a detailed understanding of STN functional neuroanatomy and network connectivity is critical to prevent the unintended neuropsychiatric and cognitive effects of stimulation at this site.

Resting-state functional connectivity is a neuroimaging tool that allows us to probe cortical (Yeo et al., 2011) and subcortical (Jung et al., 2014) brain circuits. Prior resting-state functional connectivity MRI (rs-fcMRI) studies of the STN have inconsistently revealed functional coupling with known anatomic connections. For example, prior rs-fcMRI work has not mapped the expected connectivity between STN and dorsal anterior cingulate cortex (dACC) (limbic STN), lateral orbitofrontal cortex (OFC), and prefrontal cortex (PFC) (associative STN). A small rs-fcMRI study in 14 healthy controls did not identify connectivity between STN and PFC (Brunenberg et al., 2012; Lenglet et al., 2012). Relatedly, another study that used arterial spin-labeled perfusion imaging (Fernandez-Seara et al., 2015) investigated STN resting-state functional connectivity in healthy adults, and did not report dACC and PFC connectivity. Mathys et al. (2016) mapped fcMRI in 55 healthy controls (HC) at lower spatial resolution (3.1 mm isotropic voxels), reporting anticorrelations between STN and OFC, precuneus, superior frontal gyrus (SFG), middle temporal gyrus (MTG), and cerebellum. Variance across studies is likely due to methodological differences in image acquisition and analysis. We propose that the paucity of rs-fcMRI evidence for the putative integration of STN in limbic and associative networks could primarily be attributed to limitations in brain coverage and spatial and temporal resolutions.

Increased physiological noise arising from cerebrospinal fluid (CSF) fluctuations in midline subcortical structures such as the STN is another factor that limits blood oxygenation level-dependent (BOLD) contrast-to-noise (CNR) ratio (Barry et al., 2013). Since white matter (WM) and CSF are confounding factors in fcMRI, applying higher spatial resolution minimizes partial voluming, thereby improving time series signal-to-noise ratio (tSNR) (Triantafyllou et al., 2005). High-N array coils (e.g., 32 channel head coil) maximize tSNR gains, a feature that is critical for examining the functional connectivity of small structures such as STN. However, even with a 32 channel (32Ch) head coil, it is imperative to operate in a high-resolution regime (such as 2 mm isotropic) so that there is minimal contamination of the brain parenchyma by the cardiopulmonary physiological noise,

WM, and CSF (Arnold Anteraper et al., 2013). It is noteworthy that even with multichannel array coils, the exposition of BOLD signal from the STN remains challenging as head coil sensitivity drops toward the center of the coil (Wiggins et al., 2006). Finally, to probe slow (10–100 s range) synchronous neuronal fluctuations from a small and deep subcortical structure using resting-state fcMRI, improved tSNR offered by multichannel arrays at high-spatial resolution becomes essential if not mandatory.

To address these challenges and requirements, we applied recent advances in simultaneous multislice (SMS) imaging methods (Feinberg and Setsompop, 2013). A 32-Ch phased array coil was employed with parallel imaging in the slice direction (SMS methods) so that there was no SNR penalty. The result is several fold improvement in temporal resolution fMRI without sacrificing spatial resolution or whole-brain coverage. The added benefit of faster temporal sampling using SMS imaging is improved BOLD sensitivity because of minimal aliasing of cardiac and respiratory signals, and improved statistical gains due to an increased number of BOLD time points/measurements for a given scan length.

Given the relationship between structural and functional connectivity (Hermundstad et al., 2013), and based on known neuroanatomical subdivisions of STN in nonhuman primates (Haynes and Haber, 2013), we postulated that positive functional connectivity to STN would exist in a larger subset of anatomically connected regions (in particular, dACC, lateral OFC, and PFC). Specifically, our goal was to investigate whether the STN is functionally linked to limbic, associative, and motor networks using seed-based resting-state fcMRI. To capitalize on tSNR, we used a synergistic combination of whole-brain coverage, high-spatial and temporal resolution, and multichannel array coil employing SMS imaging for data acquisition to examine STN functional connectivity.

Methods

Thirty right-handed healthy volunteers (23 females, mean age 21.7 years, age range 18–29 years) participated in the study. All participants provided written informed consent before participation in the study, in accordance with the Declaration of Helsinki. The MIT committee on the use of humans as experimental subjects review board approved the study protocol. None of the participants had a history of psychoactive medication use and neurological or psychiatric illness.

Data acquisition was performed on a Siemens 3T scanner, MAGNETOM Trio, a Tim System (Siemens AG, Healthcare Sector, Erlangen, Germany), using a commercially available radio frequency (RF) receive-only 32-Ch brain array head coil (Siemens AG, Healthcare Sector, Erlangen, Germany). The body coil was used for RF transmission. Foam cushions were used to minimize head motion. During the resting-state scan, all subjects were asked to relax in the scanner with their eyes open (staring at fixation cross). Single-shot gradient echo planar imaging (EPI), with multiband (MB) technique, was used for resting-state data collection, with an MB factor of 5. The scan duration was 10 min (two back-to-back 5 min sessions). The scan parameters used for TR/TE/flip angle/voxel size were $1000\,\text{ms}/30\,\text{ms}/61°/2 \times 2 \times 2\,\text{mm}^3$. Sixty six slices, prescribed along anterior commissure–posterior commissure (AC-PC) plane with A > P phase encode direction, were used to acquire whole-brain data (600

time points per participant). High-resolution structural scan was acquired using 3D MP-RAGE (magnetization-prepared rapid-acquisition gradient-echo) sequence. The scan parameters used for TR/TE/TI/flip angle/voxel size were 2530 ms/3.39 ms/1100 ms/7°/1.3 × 1 × 1.3 mm^3.

Data preprocessing was done using SPM8 (Friston, 2007), which for the resting state scans include motion correction, normalization with respect to the EPI template (sampling size was matched to the native 2-mm isotropic resolution) provided by SPM, and 3-mm Gaussian smoothing. Structural scan was normalized with respect to SPM's T$_1$ template. Finally, image segmentation was carried out on the T1-weighted images to yield GM, WM, and CSF masks in normalized space (Ashburner and Friston, 2005).

First-level functional connectivity analyses

Functional connectivity analysis was performed using CONN (Whitfield-Gabrieli and Nieto Castanon, 2012) toolbox. Seeds were chosen as spheres of 1 mm radius, defined around the peak co-ordinates (−8, −13.5, −7 for left STN and 11, −12.5, −7 for right STN) of the previously published atlas from 7T images (Forstmann et al., 2012). The advantage of using the hot spots from probability map-based approach for seed definition is that it captures the intersubject variability of STN more effectively. We examined the right and left STN separately since prior research has shown hemispheric differences in the nonmotor functions of STN (Eitan et al., 2013).

After band-pass filtering (0.008 < f < 0.09 Hz), denoising was carried out by using aCompcor (anatomical component-based noise correction method) (Behzadi et al., 2007) to eliminate the non-neuronal contributions from WM and CSF. Denoising step also included the regression of time points flagged as outliers due to motion, along with the seven realignment (three translation, three rotation, one composite motion) parameters and their first order derivatives. In-house custom software (nitrc.org/projects/artifact_detect/) was used for outlier detection, with thresholds of three standard deviations away from global mean for normalized signal intensity. Because of smaller voxel size, a scan-to-scan motion threshold of 0.5 mm translation and 0.5 degree rotation were used in this study. After denoising, the residual BOLD time courses from seeds (left and right STN) were extracted to obtain correlation maps. The next step was to generate Pearson's correlation coefficients between the seed time courses and the time courses of all other voxels in the brain, which were then converted to normally distributed scores using Fisher's r-to-z transform to carry out second-level general linear model analyses.

Second-level connectivity analyses

For second-level one-sample analyses, whole-brain height-level threshold of $p < 0.001$ was used for both left and right STN seeds to identify areas of significant functional connectivity. To report a cluster as statistically significant at this height threshold, a false discovery rate (FDR) corrected threshold of $p < 0.05$ was applied.

Cerebellum clusters were visualized using the SUIT toolbox for SPM (Diedrichsen, 2006; Diedrichsen et al., 2009; Diedrichsen and Zotow, 2015), and overlapped with Buckner and colleagues' (2011) 7 resting-state networks map.

Results

Statistically significant resting-state functional connectivity maps ($p < 0.001$, T > 3.40) from left and right STN seeds are shown in Figure 1. Cerebellar clusters are shown in Figure 2. FDR corrected peak clusters ($p < 0.05$) are tabulated in Table 1.

Left STN

With left STN as the seed, functional connectivity was the most significant with thalamic subregions (dorsomedial and intralaminar areas). Ventral tegmental area (VTA), bilateral anterior cingulate cortex (Brodmann area (BA) 32/ACC), and bilateral anterior and posterior insular cortex (BA 13), which form part of the limbic network, also showed significant positive correlations with left STN. Regions that showed significant positive correlations with the left STN seed also included associative and motor regions such as (a) bilateral dorsomedial PFC/presupplementary motor cortex (pre-SMA) and left opercular division of ventrolateral PFC (also known as inferior frontal gyrus [IFG]), (b) substantia nigra (SN), bilateral thalamus (ventral anterior [VA]/ventrolateral [VL] nuclei), and right posterior putamen, (c) anterior and posterior pons, and (d) left MTG/STG. Left parietal and visual association (temporoccipital) (BA 18/BA 17) cortices were also significantly correlated with left STN.

When analyzing negative correlations, left STN seed revealed two anticorrelation clusters in the cerebellum (left Crus I/Crus II and right Crus I). Both cerebellar clusters overlapped with default mode network (DMN) and fronto-parietal network representation areas, as described in Buckner et al., 2011.

Right STN

Similar to left STN, functional connectivity between right STN was the most significant within the subcortical regions, specifically the thalamic subregions (dorsomedial and intralaminar areas). Other regions that were positively correlated with right STN include hypothalamus, putamen, caudate, occipital cortices (BA 18/BA 17), BA 32/ACC, cerebellar right lobule VI/right Crus I, BA 41/BA 40, external globus pallidus (GPe), bilateral IFG/BA 44, cuneus, medial frontal gyrus/BA 10, precuneus/BA 7/BA31, right supramarginal gyrus/inferior parietal lobule, and amygdala. Of these, BA 10 and lateral OFC (BA 47) form part of the associative STN, parietal, GPe, putamen, caudate, and cerebellar regions form part of the STN motor network, pre-SMA forms part of the STN hyperdirect pathway, and insula, ACC, frontal pole, VTA, and thalamic subregions form part of the limbic STN. Insula-STN connectivity was the most robust with the left STN seed, whereas IFG-STN connectivity was the most striking with the right-STN seed. Cerebellar cluster overlapped with somatomotor, ventral attention, frontoparietal, and limbic network cerebellar representations as described in Buckner and colleagues (2011), perhaps suggesting a cerebellar contribution to the STN functional network extending beyond motor processing.

Discussion

Our primary aim was to investigate whether the functional segregation of STN into limbic, associative, and motor
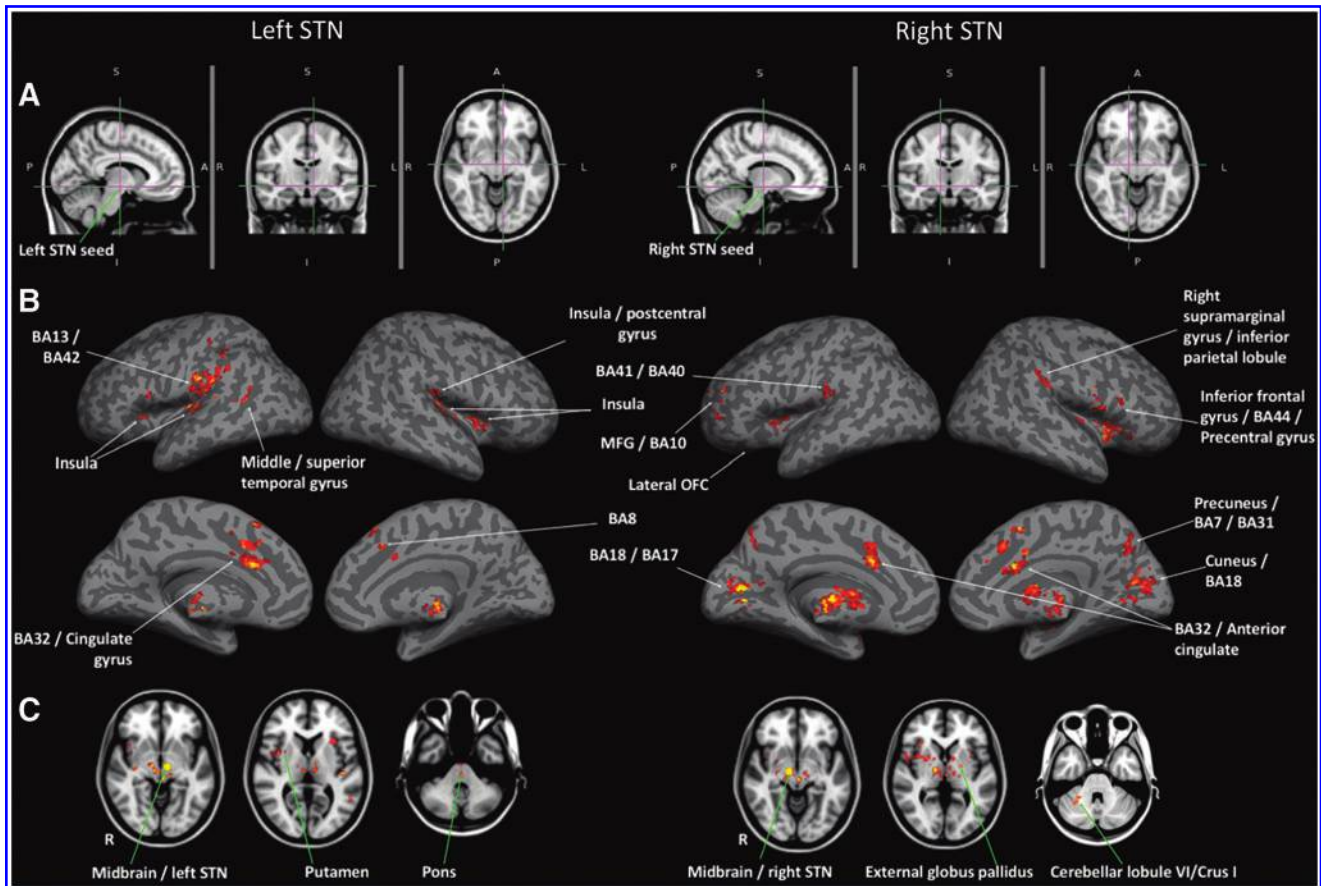
FIG. 1. Statistically significant resting-state functional connectivity maps from left and right STN (second-level analysis, $N = 30$; height threshold of whole-brain $p < 0.001$, $T_{min} = 3.4$, cluster-level threshold of $p_{FDR-corr} < 0.05$). **(A)** Left STN and right STN seeds location (MNI co-ordinates [−8, −13.5, −7] for left STN and [11, −12.5, −7] for right STN). **(B)** Cerebral cortical surface results; labels correspond to Table 1. **(C)** Subcortical volume results; labels correspond to Table 1. STN, sub-thalamic nucleus. Color images available online at www.liebertpub.com/brain

zones, previously identified by tracer studies (Haynes and Haber, 2013), would be reflected by the functional connectivity pattern of this nucleus in the human brain. We probed the functional connectivity of STN in healthy controls by optimizing resting-state fcMRI acquisition parameters to enhance spatial and temporal resolutions (Brunenburg et al., 2012; Fernandez-Seara et al., 2015; Mathys et al., 2016). We combined SMS imaging (Feinberg and Setsompop, 2013) and multichannel array coils for seed-based resting-state fcMRI of STN with a level of resolution (2 mm isotropic voxels at 1 s temporal sampling) not previously reported with whole-brain coverage. High-resolution fMRI used in combination with multichannel array coils is a technique that is well suited to identify the specificity of basal ganglia functional mapping (Anteraper et al., 2013). Our results demonstrate significant functional involvement of STN in the limbic, associative (hyperdirect/inhibitory control), and motor (indirect) networks.

Limbic network (salience network or cingulo-opercular network)

Congruent with primate tracer studies that have shown projection from dorsal ACC to medial STN (Haynes and

Haber, 2013), our findings demonstrate positive functional connectivity with both dorsal ACC and bilateral anterior and posterior insular cortices from both left and right STN seeds. Our results support the role of STN as a limbic convergence zone. Enhanced understanding of the affective neural networks that are functionally connected to the STN could bring us closer to predicting and mitigating the adverse neuropsychiatric side effects of DBS (Volkmann et al., 2010) and harnessing medial STN DBS as a putative target for treatment of obsessive compulsive disorder (Mallet et al., 2008) and addictions (Luigjes et al., 2012). A better appreciation of STN limbic subdivisions has the potential to impact clinical outcomes and surgical planning [reviewed in (Lyons, 2011)]. STN-DBS in PD has demonstrated positive influences on the motor network that result in improved bradykinesia, rigidity, and tremor. Although DBS electrodes target the motor regions of the STN, inadvertent effects on limbic STN connections may manifest as neuropsychiatric sequel, including disruptions in mood (Castrioto et al., 2014). STN-ACC and STN-insula connectivity has been previously reported, with an inverse relationship between STN-insula connectivity and the severity of motor symptoms in PD (Mathys et al., 2016). Nonmotor symptoms (NMSs) in DBS, including pain-modulating effects, could be potentially
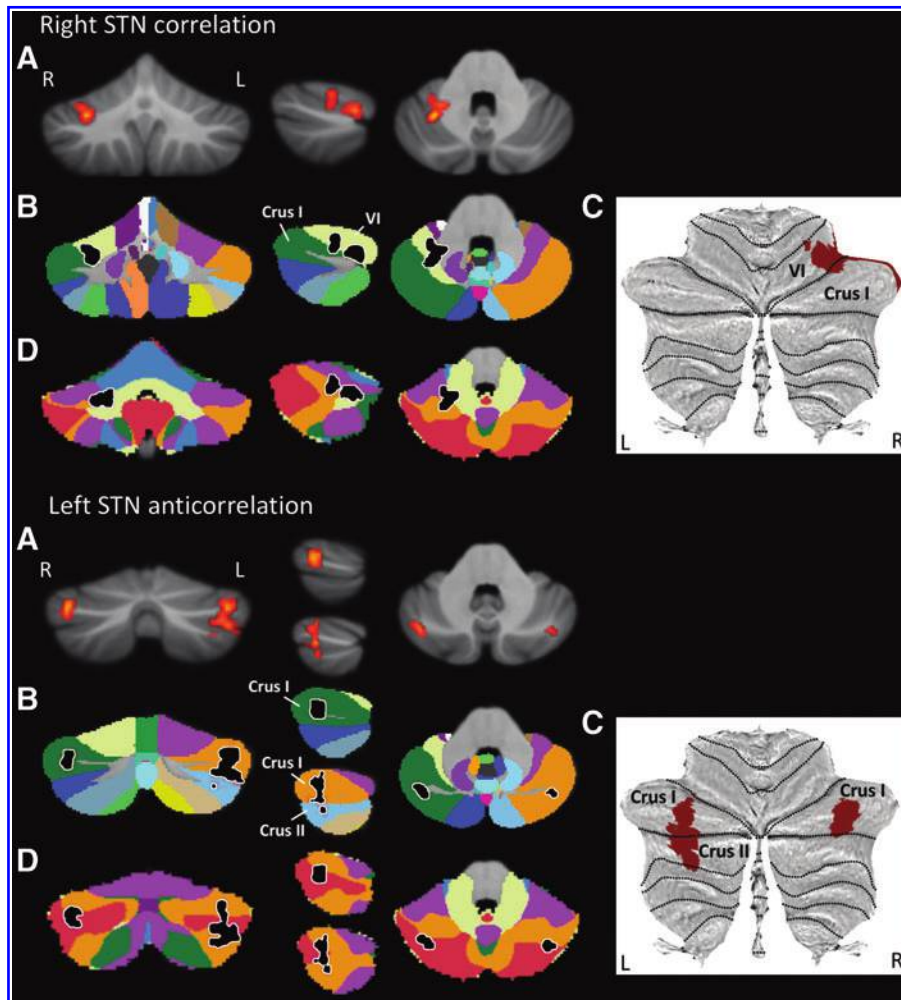
FIG. 2. Right STN correlation (top) and left STN anticorrelation clusters (bottom). **(A)** Cerebellar clusters (red) and cerebellar anatomy shown on coronal, sagittal, and axial slices through the SUIT atlas (Diedrichsen, 2006; Diedrichsen et al., 2009). **(B)** Cerebellar clusters (black with white border) and cerebellar atlas shown through the SUIT atlas; each color corresponds to a distinct cerebellar lobule; labels correspond to lobules where clusters are located. **(C)** Cerebellar clusters (red) visualized on a cerebellar flatmap (Diedrichsen and Zotow, 2015); dotted lines correspond to borders between lobules; labels correspond to lobules where clusters are located. **(D)** Cerebellar clusters (black with white border) and functional connectivity of the cerebellum based on correlations with cerebral cortical networks (Buckner et al., 2011): dark purple, visual; blue, somatomotor; green, dorsal attention; violet, ventral attention; cream, limbic; orange, frontoparietal; red, default network. R = right, L = left. SUIT, spatially unbiased infratentorial. Color images available online at www.liebertpub.com/brain

ascribed to the role of STN in the limbic network (Jung et al., 2015). Long-term follow-up studies in PD patients who underwent STN-DBS show reduction or persistence of pre-existing musculoskeletal pain and emergence of new pain (Jung et al., 2015). Significant positive correlations of hypothalamus and amgydala with right STN region of interest (ROI) revealed by our study could potentially shed light on such DBS-related homeostatic alterations in pain (Veinante et al., 2013).With the burden of NMSs evolving as a determinant in the quality of life for PD patients post-DBS, a better understanding of the limbic involvement of STN is crucial.

Our findings show positive connectivity between STN and brain regions in the limbic network, including thalamus and VTA. Bilateral STN seed ROIs unravel functional connectivity with thalamus (dorsomedial and intralaminar areas) that parallels the structural connectivity between these regions (Lambert et al., 2012). Intralaminar thalamic nucleus is involved in the limbic pathway and receives reciprocal projections with the ventral striatum (Gimenez-Amaya et al., 1995). VTA, typically associated with the limbic network, is also considered to be a part of reward circuit (Haber and Knutson, 2010) and salience network (Seeley et al., 2007). We identified VTA as functionally connected to both left and right STN seed ROIs. Connectivity between STN and VTA is consistent with alterations in reward processing after STN-DBS (Wagenbreth et al., 2015).

Associative/inhibitory control network (hyperdirect pathway)

''Life's aim is an act not a thought,'' proposed Sir Charles Sherrington (1933) to describe the centrality of action for the successful execution of a goal-directed behavior. A key component of goal-directed action requires inhibition of prepotent responses. Using stop signal inhibition tasks, human lesion and fMRI studies indicate that the STN is a key component of the action-stopping network along with right IFG, bilateral insula and pre-SMA (Aron and Poldrack, 2006; Rae et al., 2015). (Wiecki and Frank, 2013). This network is considered to be critical for a form of executive function known as inhibitory control. Human diffusion imaging studies have demonstrated cortical projections to STN from inferior and superior frontal regions (Lambert et al., 2012). An fMRI study has shown that mean diffusivity in tracts between STN and pre-SMA and between STN and IFG is correlated with stopping behavior; markers of WM structure in the tract between pre-SMA and STN are correlated with effective connectivity of the same pathway (Rae et al., 2015). Our results provide novel evidence of resting-state temporal coupling between the putative nodes of the inhibitory control network, including STN, right dorsomedial PFC, bilateral pre-SMA, and bilateral opercular divisions of ventrolateral PFC (part of IFG). We found that the left STN seed also

TABLE 1. POSITIVELY CORRELATED BRAIN REGIONS FOR LEFT AND RIGHT SUBTHALAMIC NUCLEUS
(SECOND−LEVEL ANALYSIS, $N = 30$; HEIGHT THRESHOLD OF WHOLE−BRAIN $p < 0.001$ [T = 3.4],
CLUSTER−LEVEL THRESHOLD OF $p_{FDR-corr} < 0.05$)

Brain regions	Peak cluster	Voxels per cluster	Tmax
Left STN			
Midbrain/left STN	−8 −14 −6	499	36.92
Left insula	−34 −22 10	59	6.05
Right insula	36 4 −2	175	5.85
Right insula/postcentral gyrus	42 −20 12	89	5.72
BA 32/cingulate gyrus	−8 24 26	190	5.52
BA 13/BA 42	−44 −22 8	443	5.49
Right insula	32 −26 18	42	5.27
Pons	0 −18 −36	63	5.21
Putamen	36 −18 −4	47	5.12
BA 8	4 32 56	54	4.80
Middle/superior temporal gyrus	−52 −54 6	48	4.71
Left insula	−32 20 6	43	4.61
Right STN			
Midbrain/right STN/ventral anterior nucleus	12 −12 −6	1719	37.23
BA 18/BA 17	−14 −76 12	110	7.91
BA 32/anterior cingulate	4 16 36	291	5.78
Cerebellar right lobule VI/Crus I	30 −52 −32	62	5.37
BA 41/BA 40	−48 −26 10	45	5.23
External globus pallidus/putamen	−20 −6 2	107	5.21
Right inferior frontal gyrus (IFG)/BA 44/precentral gyrus	60 10 24	72	5.16
Cuneus/BA 18	0 −78 16	316	4.93
MFG/BA 10	−36 52 24	56	4.89
Precuneus/BA 7/BA31	8 −74 44	132	4.86
Left IFG	−48 46 4	37	4.63
Right supramarginal gyrus/inferior parietal lobule	64 −32 44	106	4.40

showed connectivity with STG, a region that is associated with correct response inhibition (Rae et al., 2015).

Associative network

A primate tracer study has shown that afferents from rostral dorsomedial PFC (DPFC), including BA 10, project to portions of the STN-located ventromedial to premotor and motor projections and do not project to the medial half of STN (Haynes and Haber, 2013). Consistent with this finding, central STN stimulation in patients with DBS is associated with attentional dysfunction (Mallet et al., 2007). Our analysis revealed right STN connectivity with BA10, supporting a functional integration of STN in cognitive/associative brain networks.

Lateral OFC is considered to be part of the basal ganglia thalamocortical associative circuit (Alexander et al., 1986). We found connectivity between lateral OFC and the right STN ROI. Our results are consistent with a human PET study that has shown impaired fear recognition after STN DBS accompanied with decreased glucose metabolism in OFC (Le Jeune et al., 2008) and associative circuits (Le Jeune et al., 2010a). In contrast to the results of the present study, an fcMRI study in healthy controls (55 participants) (Mathys et al., 2016) reported OFC as negatively correlated with STN. Methodological differences in data analysis may have contributed to these divergent findings.

We found that left and right STN seed ROIs revealed positive correlations with the visual association cortex. This is consistent with previous reports using fcMRI (Mathys et al., 2016) and supports a putative role of the STN in attention (Mallet et al., 2007). Our results support involvement of

STN in visual pathways, for example, the superior colliculus-STN hyperdirect pathway (Redgrave et al., 2010).

Motor network: direct and indirect pathways

The extrapyramidal motor system is thought to be composed of two primary pathways involving the basal ganglia and the direct and indirect pathways (Lanciego et al., 2012). The direct pathway from the striatum to the internal segment of globus pallidus (GPi) facilitates movement through VA/VL thalamic excitation. In contrast, the net effect of stimulation of the indirect pathway is the inhibition of movement through VA/VL thalamic suppression. The indirect pathway involves a more circuitous information flow from the striatum to GPe, STN, and finally the GPi (Haber and Calzavara, 2009). Indirect pathway involves STN excitatory inputs to GPi and is facilitated through cortico-striato-pallido-subthalamic loops as demonstrated in stimulations studies in animals (Kolomiets et al., 2001).

The first documented patient with a lesion of STN developed unilateral flinging movements of the extremities, contralateral to the lesion, known as hemiballismus (Martin, 1927). Lesion of the STN involves loss of motor suppression or "tone" of the indirect pathway, resulting in exaggerated involuntary movements (Lozano, 2001). Our results show functional connectivity between right STN and components of the indirect pathway, including GP (external and internal segments), thalamus (VA/VL nuclei), and striatum (putamen and caudate). With the seed ROI from left STN, functional connectivity with bilateral thalamus (VA/VL nuclei) and right putamen was revealed. VA/VL nuclei are linked with

motor cortices based on studying the clinical syndromes resulting from thalamic infarction in humans (Schmahmann, 2003). Reciprocally connected excitatory (glutamatergic) neurons of the STN and inhibitory (GABAergic) neurons of the GPe are critical components of the indirect pathway (Plenz and Kital, 1999). The STN-GPe system is a central pacemaker of the basal ganglia, and a disturbance of the balance of excitation and inhibition between these structures is thought to contribute to the motor symptoms of PD (Bevan et al., 2002; Plenz and Kital, 1999). Although we identified positive functional connectivity between right STN and GPe, our results do not capture the complexity of this relationship. Since the release of inhibitory and excitatory transmitters are energy-consuming processes, neuronal inhibitory activity may contribute to the BOLD signal (Arthurs and Boniface, 2002). Thus, complementary imaging and electrophysiological techniques would be necessary to fully understand the influence of afferent inhibitory pathways to STN.

Motor network: other contributions

We identified functional connectivity between STN and other components of the motor network such as SN, cerebellum, and parietal lobes. SN is a key input and output to the basal ganglia involved in motor control and is affected in PD (Cosottini et al., 2014). Anatomical evidence for the two-way (bisynaptic) communication between STN and cerebellum has been shown in cebus monkeys (Bostan et al., 2010). There is electrophysiological evidence of cerebellar activity during STN-DBS (Sutton et al., 2015). Our results showed left-STN functional connectivity with the pons. This finding is congruent with rodent and primate tracer studies that have shown structural connectivity between STN and the pedunculopontine nucleus and between STN and the locus coeruleus (Carpenter et al., 1981; Hammond et al., 1983). In PD patients, combined pedunculopontine-STN stimulation has shown improved motor control, particularly for gait and axial symptoms (Khan et al., 2012; Stefani et al., 2007).

The right STN revealed significant connectivity with right supramarginal and inferior parietal regions consistent with previous resting-state fMRI connectivity studies (Brunenberg et al., 2012; Mathys et al., 2016). There is electrophysiological and functional neuroimaging evidence that STN DBS in PD patients modulates cortical motor network activity and is associated with desynchronization of cortical activity in bilateral parietal areas (Weiss et al., 2015a, 2015b).

STN–cerebellum connectivity: nonmotor considerations

A sizeable body of anatomical (Kelly and Strick, 2003; Middleton and Strick, 1994; Schmahmann and Pandya, 1997), behavioral (Guell et al., 2015; Hoche et al., 2016; Levisohn et al., 2000; Ravizza et al., 2009; Riva and Giorgi, 2000; Schmahmann and Sherman, 1998; Thompson and Steinmetz, 2009), and neuroimaging evidence (Halko et al., 2014; Keren-Happuch et al., 2014; Stoodley and Schmahmann, 2009; Stoodley et al., 2012) supports a role of the cerebellum not only in motor control but also in cognitive and affective processes. Our discussion of STN–cerebellar connectivity must consider, accordingly, the possibility of cerebellar contributions to the STN networks that extend beyond motor control.

Right STN seed analysis revealed a cluster of positive correlation in right cerebellar lobule VI/Crus I. Several observations indicate that the functional significance of this cluster may not be confined to the motor realm. Two motor representations have been recognized in the cerebellum since the work of Snider and Eldred: one in lobules IV/V/VI and one in lobule VIII (Bushara et al., 2001; Grodd et al., 2001; see also Rijntjes et al., 1999; Snider and Eldred, 1952; Takanashi et al., 2003; Thickbroom et al., 2003). Although our right STN seed cerebellar cluster occupies lobule VI, its location is confined to the *caudal* portions of this lobule (Fig. 2B, C). The fact that lobule VI motor representation has been consistently identified in the *rostral* aspect of lobule VI, together with the fact that our cluster extends to Crus I, suggests that this correlation might be at least partially related to nonmotor information processing. This notion is further supported when overlapping our right STN–cerebellar cluster with Buckner's 7 resting-state networks (Buckner et al., 2011). Buckner and colleagues applied a winner-takes-all algorithm to determine the strongest functional correlation of each cerebellar voxel to one of the seven cerebral cortical resting-state networks defined in Yeo and colleagues (2011). When viewing our cluster within this framework, an overlap can be appreciated with somatomotor, ventral attention, frontoparietal, and limbic network cerebellar representations (Fig. 2D, top).

Left STN seed analysis showed two clusters of negative correlation, one in left cerebellar Crus I/Crus II and one in right cerebellar Crus I (Fig. 2A–C). It has been firmly established by anatomical (Kelly and Strick, 2003; Schmahmann and Pandya, 1997), clinical (Schmahmann et al., 2009; Stoodley et al., 2016), and neuroimaging studies (Keren-Happuch et al., 2014; Stoodley and Schmahmann, 2009; Stoodley et al., 2012) that motor representations in the cerebellum do not map to Crus I/Crus II. In addition, Crus I/Crus II fMRI activity has been observed in multiple nonmotor tasks, including working memory, language social, and emotion processing (Keren-Happuch et al., 2014; Stoodley and Schmahmann, 2009; Stoodley et al., 2012). Furthermore, we observed an overlap between these clusters and cerebellar DMN representations (also encroaching frontoparietal network areas) (Fig. 2D).

Right STN seed *positive* cerebellar correlations might appear at odds with left STN seed *negative* cerebellar correlations. However, patterns of positive and negative correlations between nonmotor processing areas have been described in the cerebral hemispheres—some nonmotor regions (DMN, ''task-negative'') characteristically anticorrelate with other (''task-positive'') nonmotor areas (Fox et al., 2005). Perhaps coherently, cerebellar anticorrelations were observed only in those clusters that overlapped with cerebellar DMN areas in our analysis.

This observation further supports the notion that our STN–cerebellar findings, including both positive and negative correlations, might correspond to channels of information processing extending beyond motor control. Nonmotor cerebellar contributions to the STN networks become entirely logical in the context of STN connectivity with limbic, associative, and motor networks described in this study, as well as with previous tract tracing observations linking the cerebellum with both sensorimotor and associative STN territories (Bostan et al., 2010). Taken together, it is reasonable to consider that STN–cerebellar connectivity integrates basal ganglia and cerebellar functions in both motor and nonmotor domains.

Future work

Using resting-state fcMRI, we demonstrated the tripartite network coupling of the STN (correlations with limbic, associative, and motor networks). However, resolution limitations prevented us from specifically examining individual subdivisions within STN itself. A combination of ultrahigh field strength (7 T), higher spatial resolution (1 mm^3), and multichannel arrays with SMS and whole-brain imaging could be used in the future to minimize contamination of STN voxels with the BOLD signals from neighboring structures such as thalamus and lateral hypothalamus. 7 T and ultrahigh-spatial resolution have already been proposed (de Hollander et al., 2015) to alleviate the ''cocktail problem'' to gather unmixed signals from STN and the adjacent SN. Harnessing methodological advances might enable voxel-to-voxel functional connectivity analysis to be carried out in an attempt to parse out putative lateral/medial segregation of motor and limbic networks, thereby interrogating possible functional gradients within STN. Enhanced functional anatomical understanding of STN could potentially refine the clinical applications of DBS by separating the target region and avoiding complications such as neuropsychiatric disorders and pain.

Anatomic segregation of GABA and glutamatergic STN outputs has been described previously (Levesque and Parent, 2005); however, defining excitatory or inhibitory outputs from STN is beyond the scope of this study. Valuable insights into the functional underpinnings of STN could be gained by adopting multimodality (PET–fcMRI) approaches. In particular, high-resolution MRI could benefit PET research by providing effective atlases for registration while allowing further characterization of neuropsychiatric side effects imparted by STN-DBS (Mallet et al., 2007). Finally, diffusion-weighted imaging can be combined with fcMRI to perform anatomically defined functional subparcellation of STN efferent and afferent WM tracts. Such methods have been successfully employed for exploring thalamic connectivity (O'Muircheartaigh et al., 2015) and could be extended to composite structures such as STN [e.g., (Fan et al., 2016)].

Previous resting-state fcMRI studies have not shown STN-IFG or STN-STG connectivity (Fernandez-Seara et al., 2015; Mathys et al., 2016). In contrast to prior work that employed 12-Ch head coils, this study takes advantage of 32-Ch array head coils. Our previous work has shown that increasing the number of RF receiver channels in array coils from 12 Ch to 32 Ch outperforms the 12-Ch coil by a factor of $2.3\times$ averaged over the given signal area (Anteraper et al., 2013). Furthermore, in comparison with the 12-Ch coil, the peripheral cortex SNR and central SNR were improved by a factor of $1.4\times$ and $2.7\times$, respectively, exhibiting the increased sensitivity offered by the 32-Ch coil not only at the cortex but also at deeper structures and subcortical areas. Combination of SMS and high-spatiotemporal resolution EPI for statistical power enhancements in BOLD sensitivity has also previously been demonstrated (Arnold Anteraper et al., 2014). Systematic evaluation of the potential methodological benefit of high-resolution imaging using the 32-Ch head coil on BOLD CNR in the STN, particularly in the susceptibility-prone temporal and mid-brain regions, is beyond the scope of this study.

Conclusions

Using a combination of recent advances in SMS, multi-channel array coils, and high-resolution imaging, we identified resting-state functional connectivity of the STN with limbic, associative, and motor networks. It is critical to delineate the functional heterogeneity of STN to reduce the neuropsychiatric complications of electrical stimulation with DBS. This work contributes to the enhanced understanding of the role of basal ganglia substructures in cognition, emotion, motivation, and motor functions.

Disclosure Statement

No competing financial interests exist.

References

Alexander GE, DeLong MR, Strick PL. 1986. Parallel organization of functionally segregated circuits linking basal ganglia and cortex. Annu Rev Neurosci 9:357–381.

Anteraper SA, Whitfield-Gabrieli S, Keil B, Shannon S, Gabrieli JD, Triantafyllou C. 2013. Exploring functional connectivity networks with multichannel brain array coils. Brain Connect 3:302–315.

Arnold Anteraper S, Whitfield-Gabrieli S, Geddes M, Triantafyllou C, Gabrieli JD, Mattfeld A. Functional Connectivity Differences of the Anterior and Posterior Entorhinal Cortex in Humans, Society for Neuroscience, Annual Meeting, Washington: DC, USA, 2014.

Aron AR, Poldrack RA. 2006. Cortical and subcortical contributions to Stop signal response inhibition: role of the subthalamic nucleus. J Neurosci 26:2424–2433.

Arthurs OJ, Boniface S. 2002. How well do we understand the neural origins of the fMRI BOLD signal? Trends Neurosci 25:27–31.

Ashburner J, Friston KJ, 2005. Unified segmentation. Neuroimage 26:839–851.

Barry RL, Coaster M, Rogers BP, Newton AT, Moore J, Anderson AW, et al. 2013. On the origins of signal variance in FMRI of the human midbrain at high field. PLoS One 8:e62708.

Behzadi Y, Restom K, Liau J, Liu TT. 2007. A component based noise correction method (CompCor) for BOLD and perfusion based fMRI. Neuroimage 37:90–101.

Benabid AL, Chabardes S, Mitrofanis J, Pollak P. 2009. Deep brain stimulation of the subthalamic nucleus for the treatment of Parkinson's disease. Lancet Neurol 8:67–81.

Bevan MD, Magill PJ, Terman D, Bolam JP, Wilson CJ. 2002. Move to the rhythm: oscillations in the subthalamic nucleus-external globus pallidus network. Trends Neurosci 25:525–531.

Bostan AC, Dum RP, Strick PL. 2010. The basal ganglia communicate with the cerebellum. Proc Natl Acad Sci U S A 107:8452–8456.

Brunenberg EJL, Moeskops P, Backes WH, Pollo C, Cammoun L, Vilanova A, et al. 2012. Structural and resting state functional connectivity of the subthalamic nucleus: identification of motor STN parts and the hyperdirect pathway. PLoS One 7:e39061.

Buckner RL, Krienen FM, Castellanos A, Diaz JC, Yeo BT. 2011. The organization of the human cerebellum estimated by intrinsic functional connectivity. J Neurophysiol 106: 2322–2345.

Bushara KO, Wheat JM, Khan A, et al. 2001. Multiple tactile maps in the human cerebellum. Neuroreport 12:2483–2486.

Carpenter MB, Carleton SC, Keller JT, Conte P. 1981. Connections of the subthalamic nucleus in the monkey. Brain Res 224:1–29.

Castrioto A, Lhommee E, Moro E, Krack P. 2014. Mood and behavioural effects of subthalamic stimulation in Parkinson's disease. Lancet Neurol 13:287–305.

Cosottini M, Frosini D, Pesaresi I, Costagli M, Biagi L, Ceravolo R, et al. 2014. MR imaging of the substantia nigra at 7 T enables diagnosis of Parkinson disease. Radiology 271:831–838.

de Hollander G, Keuken MC, Forstmann BU. 2015. The subcortical cocktail problem; mixed signals from the subthalamic nucleus and substantia nigra. PLoS One 10:e0120572.

Diedrichsen J, Balsters JH, Flavell J, Cussans E, Ramnani N. 2009. A probabilistic MR atlas of the human cerebellum. Neuroimage 46:39–46.

Diedrichsen J, Zotow E. 2015. Surface-based display of volume-averaged cerebellar imaging data. PLoS One 10:e0133402.

Diedrichsen J. 2006. A spatially unbiased atlas template of the human cerebellum. Neuroimage 33:127–138.

Eitan R, Shamir RR, Linetsky E, Rosenbluh O, Moshel S, Ben-Hur T, et al. 2013. Asymmetric right/left encoding of emotions in the human subthalamic nucleus. Front Syst Neurosci 7:1–11.

Fan Q, Witzel T, Nummenmaa A, Van Dijk KR, Van Horn JD, Drews MK, et al. 2016. MGH-USC human connectome project datasets with ultra-high b-value diffusion MRI. Neuroimage 124(Pt B):1108–1114.

Feinberg DA, Setsompop K. 2013. Ultra-fast MRI of the human brain with simultaneous multi-slice imaging. J Magn Reson 229:90–100.

Fernandez-Seara MA, Mengual E, Vidorreta M, Castellanos G, Irigoyen J, Erro E, Pastor MA. 2015. Resting state functional connectivity of the subthalamic nucleus in Parkinson's disease assessed using arterial spin-labeled perfusion fMRI. Hum Brain Mapp 36:1937–1950.

Forstmann BU, Keuken MC, Jahfari S, Bazin PL, Neumann J, Schafer A, et al. 2012. Cortico-subthalamic white matter tract strength predicts interindividual efficacy in stopping a motor response. Neuroimage 60:370–375.

Fox MD, Snyder AZ, Vincent JL, Corbetta M, Van essen DC, Raichle ME. 2005. The human brain is intrinsically organized into dynamic, anticorrelated functional networks. Proc Natl Acad Sci USA 102:9673–9678.

Friston KJ. 2007. *Statistical Parametric Mapping: The Analysis of Funtional Brain Images*. Amsterdam; Boston: Elsevier/Academic Press. vii, 647 p., [32] p. of plates p.

Gimenez-Amaya JM, McFarland NR, de las Heras S, Haber SN. 1995. Organization of thalamic projections to the ventral striatum in the primate. J Comp Neurol 354:127–149.

Greenhouse I, Gould S., Houser M, Hicks G, Gross J, Aron A. 2011. Stimulation at dorsal and ventral electrode contacts targeted at the subthalamic nucleus has different effects on motor and emotion functions in Parkinson's disease. Neuropsychologia 49:528–534.

Grodd W, Hülsmann E, Lotze M, Wildgruber D, Erb M. 2001. Sensorimotor mapping of the human cerebellum: fMRI evidence of somatotopic organization. Hum Brain Mapp 13: 55–73.

Guell X, Hoche F, Schmahmann JD. 2015. Metalinguistic deficits in patients with cerebellar dysfunction: empirical support for the dysmetria of thought theory. Cerebellum 14:50–58.

Haber SN, Calzavara R. 2009. The cortico-basal ganglia integrative network: the role of the thalamus. Brain Res Bull 78:69–74.

Haber SN, Knutson B. 2010. The reward circuit: linking primate anatomy and human imaging. Neuropsychopharmacology 35:4–26.

Halko MA, Farzan F, Eldaief MC, Schmahmann JD, Pascual-Leone A. 2014. Intermittent theta-burst stimulation of the lateral cerebellum increases functional connectivity of the default network. J Neurosci 34: 12049–12056.

Hammond C, Rouzaire-Dubois B, Feger J, Jackson A, Crossman AR. 1983. Anatomical and electrophysiological studies on the reciprocal projections between the subthalamic nucleus and nucleus tegmenti pedunculopontinus in the rat. Neuroscience 9:41–52.

Hartmann CJ, Chaturvedi A, Lujan JL. 2015. Quantitative analysis of axonal fiber activation evoked by deep brain stimulation via activation density heat maps. Front Neurosci 9:28.

Haynes WI, Haber SN. 2013. The organization of prefrontal-subthalamic inputs in primates provides an anatomical substrate for both functional specificity and integration: implications for Basal Ganglia models and deep brain stimulation. J Neurosci 33:4804–4814.

Hermundstad AM, Bassett DS, Brown KS, Aminoff EM, Clewett D, Freeman S, et al. 2013. Structural foundations of resting-state and task-based functional connectivity in the human brain. Proc Natl Acad Sci USA 110:6169–6174.

Hoche F, Guell X, Sherman JC, Vangel MG, Schmahmann JD. 2016. Cerebellar contribution to social cognition. Cerebellum 15:732–743.

Jung WH, Jang JH, Park JW, Kim E, Goo EH, Im OS, Kwon JS. 2014. Unravelling the intrinsic functional organization of the human striatum: a parcellation and connectivity study based on resting-state FMRI. PLoS One 9:e106768.

Jung YJ, Kim HJ, Jeon BS, Park H, Lee WW, Paek SH. 2015. An 8-year follow-up on the effect of subthalamic nucleus deep brain stimulation on pain in Parkinson disease. JAMA Neurol 72:504–510.

Kelly RM, Strick PL. 2003. Cerebellar loops with motor cortex and prefrontal cortex of a nonhuman primate. J Neurosci 23: 8432–8444.

Keren-Happuch E, Chen SH, Ho MH, Desmond JE. 2014. A meta-analysis of cerebellar contributions to higher cognition from PET and fMRI studies. Hum Brain Mapp 35:593–615.

Khan S, Gill SS, Mooney L, White P, Whone A, Brooks DJ, Pavese N. 2012. Combined pedunculopontine-subthalamic stimulation in Parkinson disease. Neurology 78:1090–1095.

Kolomiets BP, Deniau JM, Mailly P, Menetrey A, Glowinski J, Thierry AM. 2001. Segregation and convergence of information flow through the cortico-subthalamic pathways. J Neurosci 21:5764–5772.

Lambert C, Zrinzo L, Nagy Z, Lutti A, Hariz M, Foltynie T, et al. 2012. Confirmation of functional zones within the human subthalamic nucleus: patterns of connectivity and sub-parcellation using diffusion weighted imaging. Neuroimage 60:83–94.

Lanciego JL, Luquin N, Obeso JA. 2012. Functional neuroanatomy of the basal ganglia. Cold Spring Harbor Perspect Med 2:a009621.

Le Jeune F, Peron J, Biseul I, Fournier S, Sauleau P, Drapier S, et al. 2008. Subthalamic nucleus stimulation affects orbitofrontal cortex in facial emotion recognition: a PET study. Brain 131:1599–1608.

Le Jeune F, Peron J, Grandjean D, Drapier S, Haegelen C, Garin E, et al. (2010a) Subthalamic nucleus stimulation affects limbic and associative circuits: a PET study. Eur J Nucl Med Mol Imaging 37:1512–1520.

Lenglet C, Abosch A, Yacoub E, De Martino F, Sapiro G, Harel N. 2012. Comprehensive in vivo mapping of the human basal ganglia and thalamic connectome in individuals using 7T MRI. PLoS One 7:e29153.

Levesque JC, Parent A. 2005. GABAergic interneurons in human subthalamic nucleus. Mov Disord 20:574–584.

Levisohn L, Cronin-Golomb A, Schmahmann JD. 2000. Neuropsychological consequences of cerebellar tumour resection in children: cerebellar cognitive affective syndrome in a paediatric population. Brain 123:1041–1050.

Lozano AM. 2001. The subthalamic nucleus: myth and opportunities. Mov Disord 16:183–184.

Luigjes J, van den Brink W, Feenstra M, van den Munckhof P, Schuurman PR, Schippers R, et al. 2012. Deep brain stimulation in addiction: a review of potential brain targets. Mol Psychiatry 17:572–583.

Lyons MK. 2011. Deep brain stimulation: current and future clinical applications. Mayo Clin Proc 86:662–672.

Mallet L, Polosan M, Jaafari N, Baup N, Welter ML, Fontaine D, et al. 2008. Subthalamic nucleus stimulation in severe obsessive-compulsive disorder. N Engl J Med 359:2121–2134.

Mallet L, Schupbach M, N'Diaye K, Remy P, Bardinet E, Czernecki V, et al. 2007. Stimulation of subterritories of the subthalamic nucleus reveals its role in the integration of the emotional and motor aspects of behavior. Proc Natl Acad Sci U S A 104:10661–10666.

Martin JP. 1927. Hemichorea resulting from a local lesion of the brain (the syndrome of the body of Luys). Brain 50:637–651.

Mathys C, Caspers J, Langner R, Sudmeyer M, Grefkes C, Reetz K, et al. 2016. Functional connectivity differences of the subthalamic nucleus related to Parkinson's disease. Hum Brain Mapp 37:1235–1253.

Mavridis I, Boviatsis E, Anagnostopoulou S. 2013. Anatomy of the human subthalamic nucleus: a combined morphometric study. Anat Res Int 2013:319710.

Middleton FA, Strick PL. 1994. Anatomical evidence for cerebellar and basal ganglia involvement in higher cognitive function. Science 266:458–461.

O'Muircheartaigh J, Keller SS, Barker GJ, Richardson MP. 2015. White matter connectivity of the thalamus delineates the functional architecture of competing thalamocortical systems. Cereb Cortex 25:4477–4489.

Plenz D, Kital ST. 1999. A basal ganglia pacemaker formed by the subthalamic nucleus and external globus pallidus. Nature 400:677–682.

Rae CL, Hughes LE, Anderson MC, Rowe JB. 2015. The prefrontal cortex achieves inhibitory control by facilitating subcortical motor pathway connectivity. J Neurosci 35: 786–794.

Ravizza SM, Mccormick CA, Schlerf JE, Justus T, Ivry RB, Fiez JA. 2006. Cerebellar damage produces selective deficits in verbal working memory. Brain 129:306–320.

Redgrave P, Coizet V, Comoli E, McHaffie JG, Leriche M, Vautrelle N, et al. 2010. Interactions between the midbrain superior colliculus and the basal ganglia. Front Neuroanat 4: pii: 132.

Rijntjes M, Buechel C, Kiebel S, Weiller C. 1999. Multiple somatotopic representations in the human cerebellum. Neuroreport 10:3653–3658

Riva D, Giorgi C. 2000. The cerebellum contributes to higher functions during development: evidence from a series of children surgically treated for posterior fossa tumours. Brain 123: 1051–1061.

Scangos KW, Shahlaie K. 2017. Acute frequency-dependent hypomania induced by ventral subthalamic nucleus deep brain stimulation in Parkinson's Disease: a case report. Biol Psychiatry 82:e39–e41.

Schmahmann JD, Macmore J, Vangel M. 2009. Cerebellar stroke without motor deficit: clinical evidence for motor and non-motor domains within the human cerebellum. Neuroscience 162:852–861.

Schmahmann JD, Pandya DN. 1997. The cerebrocerebellar system. Int Rev Neurobiol 41:31–60.

Schmahmann JD, Sherman JC. 1998. The cerebellar cognitive affective syndrome. Brain 121:561–579.

Schmahmann JD. 2003. Vascular syndromes of the thalamus. Stroke 34:2264–2278.

Seeley WW, Menon V, Schatzberg AF, Keller J, Glover GH, Kenna H, et al. 2007. Dissociable intrinsic connectivity networks for salience processing and executive control. J Neurosci 27:2349–2356.

Sherrington C. The Brain and its mechanism. Cambridge: Cambridge University Press; 1933.

Sieger T, Serranova T, Fuzicka F, Vostatek P, Wild J, Stastna D, et al. 2015. Distinct populations of neurons respond to emotional valence and arousal in the human subthalamic nucleus. PNAS 112:3116–3121.

Snider RS, Eldred E. 1952. Cerebrocerebellar relationships in the monkey. J Neurophysiol 15:27–40.

Stefani A, Lozano AM, Peppe A, Stanzione P, Galati S, Tropepi D, et al. 2007. Bilateral deep brain stimulation of the pedunculopontine and subthalamic nuclei in severe Parkinson's disease. Brain 130:1596–1607.

Stoodley CJ, Macmore JP, Makris N, Sherman JC, Schmahmann JD. 2016. Location of lesion determines motor vs. cognitive consequences in patients with cerebellar stroke. Neuroimage Clin 12:765–775.

Stoodley CJ, Schmahmann JD. 2009. Functional topography in the human cerebellum: a meta-analysis of neuroimaging studies. Neuroimage 44:489–501

Stoodley CJ, Valera EM, Schmahmann JD. 2012. Functional topography of the cerebellum for motor and cognitive tasks: an fMRI study. Neuroimage 59:1560–1570.

Sutton AC, O'Connor KA, Pilitsis JG, Shin DS. 2015. Stimulation of the subthalamic nucleus engages the cerebellum for motor function in parkinsonian rats. Brain Struct Funct 220:3595–3609.

Takanashi M, Abe K, Yanagihara T, et al. 2003. A functional MRI study of somatotopic representation of somatosensory stimulation in the cerebellum. Neuroradiology 45:149–152.

Temel Y, Kessels A, Tan S, Topdag A, Boon P, Visser-Vandewalle V. 2006. Behavioural changes after bilateral subthalamic stimulation in advanced Parkinson disease: a systematic review. Parkinonism Relat Disord 12:265–272.

Thickbroom GW, Byrnes ML, Mastaglia FL. 2003. Dual representation of the hand in the cerebellum: activation with

voluntary and passive finger movement. Neuroimage 18: 670–674.

Thompson RF, Steinmetz JE. 2009. The role of the cerebellum in classical conditioning of discrete behavioral responses. Neuroscience 162:732–755.

Triantafyllou C, Hoge RD, Krueger G, Wiggins CJ, Potthast A, Wiggins GC, Wald LL. 2005. Comparison of physiological noise at 1.5 T, 3 T and 7 T and optimization of fMRI acquisition parameters. Neuroimage 26:243–250.

Ulla M, Thobois S, Llorca PM, Derost P, Lemaire JJ, Chereau-Boudet I, et al. 2011. Contact dependent reproducible hypomania induced by deep brain stimulation in Parkinson's disease: clinical, anatomical and functional imaging study. J Neurol Neurosurg Psychiatry 82:607–614.

Veinante P, Yalcin I, Barrot M. 2013. The amygdala between sensation and affect: a role in pain. J Mol Psychiatry 1:9.

Volkmann J, Daniels C, Witt K. 2010. Neuropsychiatric effects of subthalamic neurostimulation in Parkinson disease. Nat Rev Neurol 6:487–498.

Voon V, Krack P, Lang AE, Lozano AM, Dujardin K, Schupbach M, et al. 2008. A multicenter study on suicide outcomes following subthalamic stimulation for Parkinson's disease. Brain 131:2720–2728.

Wagenbreth C, Zaehle T, Galazky I, Voges J, Guitart-Masip M, Heinze HJ, Duzel E. 2015. Deep brain stimulation of the subthalamic nucleus modulates reward processing and action selection in Parkinson patients. J Neurol 262:1541–1547.

Weiss D, Klotz R, Govindan RB, Scholten M, Naros G, Ramos-Murguialday A, et al. (2015a) Subthalamic stimulation modulates cortical motor network activity and synchronization in Parkinson's disease. Brain 138:679–693.

Weiss PH, Herzog J, Potter-Nerger M, Falk D, Herzog H, Deuschl G, et al. (2015b) Subthalamic nucleus stimulation improves parkinsonian gait via brainstem locomotor centers. Mov Disord 30:1121–1125.

Whitfield-Gabrieli S, Nieto Castanon A. 2012. Conn: a functional connectivity toolbox for correlated and anticorrelated brain networks. Brain Connect 2:125–141.

Wiecki TV, Frank MJ. 2013. A computational model of inhibitory control in frontal cortex and basal ganglia. Psychol Rev 120:329–355.

Wiggins GC, Triantafyllou C, Potthast A, Reykowski A, Nittka M, Wald LL. 2006. 32-channel 3 Tesla receive-only phased-array head coil with soccer-ball element geometry. Magn Reson Med 56:216–223.

Witt K, Daniels C, Reiff J, Krack P, Volkmann J, Pinsker MO, et al. 2008. Neuropsychological and psychiatric changes after deep brain stimulation for Parkinson's disease: a randomized, multicenter study. Lancet Neurol 7:605–614.

Yeo BT, Krienen FM, Sepulcre J, Sabuncu MR, Lashkari D, Hollinshead M, et al. 2011. The organization of the human cerebral cortex estimated by intrinsic functional connectivity. J Neurophysiol 106:1125–1165.

Address correspondence to:
Sheeba Arnold Anteraper
A. A. Martinos Imaging Center
McGovern Institute for Brain Research
Massachusetts Institute of Technology
77 Massachusetts Avenue, Bldg. 46, Room 46-1171
Cambridge, MA 02139

E-mail: sheeba@mit.edu